de Haas–van Alphen measurements of the scattering of conduction electrons from hydrogen in copper

W. R. Wampler* and B. Lengeler
Institut für Festkörperforschung der Kernforschungsanlage Jülich, D 5170 Jülich, Germany
(Received 24 January 1977)

de Haas–van Alphen Dingle temperatures for the scattering of conduction electrons from hydrogen in copper have been measured for the first time in a metal-hydrogen system. Special care was attributed to the sample preparation to ensure a random distribution of the hydrogen in the copper lattice. The strongest scattering rates are observed at the necks of the Fermi surface and the weakest in the belly regions ⟨100⟩ being smaller here by a factor of 3.3. The observed anisotropy of the scattering gives strong indication that the hydrogen occupies octahedral interstices in the fcc copper lattice. The data have been analyzed in terms of Friedel phase shifts according to a theory by Holzwarth and Lee. The s phase shift is the dominant one, the p phase shift is about an order of magnitude smaller and the d phase shifts are negligible. This is a consequence of the short range of the hydrogen potential located at an octahedral interstice. Backscattering is found to give an essential contribution to the Friedel phase shifts. A recent average-t-matrix approximation (ATA) calculation for CuH by Huisman and Weiss predicts scattering rates in excellent agreement with the experiment. The descriptions of the electron scattering by ATA and by phase-shift analysis are compared for CuH. A model calculation is proposed which allows to find out how far backscattering is included in the ATA calculations.

I. INTRODUCTION

The de Haas–van Alphen (dHvA) effect provides one of the most powerful experimental techniques to investigate the electronic structure of pure metals, ordered metallic compounds, and dilute alloys. Besides the determination of Fermi surfaces and cyclotron masses the effect has been used in recent years to obtain detailed information on the scattering of the conduction electrons from impurity atoms.[1] In fact, from Dingle-temperature measurements the reciprocal lifetime or scattering rate $1/\tau^*(\vec{k})$ of the electrons in a Bloch state can be determined locally over the Fermi surface. The scattering rate is usually anisotropic depending on the type of defect, on its position, and on the host lattice. Up to now the dHvA effect has been used to investigate the scattering from various substitutional defects in noble-metal hosts.[2–5] In this paper we will report on measurements of the electron scattering from interstitial hydrogen in copper. It is the first investigation of that kind on a metal-hydrogen system. It will be shown that the hydrogen is a strong scattering center in copper and that the scattering rates show a pronounced anisotropy which is essentially determined by the location of the hydrogen at octahedral interstitial lattice sites.

Section II describes how the dHvA effect can be used to determine scattering rates. In Sec. III the details of the experiment and the experimental results are given. In Sec. IV the anisotropy and magnitude of the scattering rates of electrons from hydrogen in Cu are discussed in the frame of a phase-shift analysis and of an average-t-matrix approximation (ATA) calculation.

II. METHOD

The dHvA effect and its use to investigate the electron scattering from defects is discussed in detail in review articles by Gold[6] and Springford.[1] The following discussion gives a brief account of the essential aspects.

The dHvA effect is the oscillatory variation of the magnetization of a metal with the magnetic field H. The component of the oscillatory magnetization parallel to the field can be expressed as (for one extremal cross section and no higher dHvA harmonics):

$$M = A(T, H, X^*)\sin(2\pi F/H + \beta)\,, \tag{1}$$

$$A = A_0(H, X^*)(bm_c^* T/m_0 H)[\sinh(bm_c^* T/m_0 H)]^{-1}, \tag{2}$$

$$A_0 = D\sqrt{H}\cos(\pi g_c^* m_c^*/2m_0)\exp(-bm_c^* X^*/m_0 H), \tag{3}$$

where D and β are constants for a given orbit. The magnetization varies periodically in $1/H$ with the dHvA frequency $F = \hbar c A_{ex}/2\pi e$, where A_{ex} is the extremal cross-sectional area of the Fermi surface normal to $\vec{H}$. The constant b has the value 14.6925 T/K. m_c^* and m_0 are the cyclotron and the free-electron masses. Of special interest in this paper is the Dingle temperature X^* which describes the broadening of the Landau levels due to the scattering of the conduction electrons at defects. g_c^* is the spin splitting g factor. Quantities with an asterisk are renormalized for electron-phonon interaction as is explained below.

As a result of the high phase $2\pi F/H$ of the oscillations for typical experimental conditions only those electrons in a narrow band around the extremal cross section contribute to the dHvA signal. Therefore, all quantities derived from dHvA measurements are orbital averages around the extremal cross sections. The Dingle temperatures are orbital averages, denoted in the following by $\langle\ \rangle$, of the local scattering rates $1/\tau^*(\vec{k})$:

$$X^* = (\hbar/2\pi k_B)\langle 1/\tau^*(\vec{k})\rangle . \tag{4}$$

The Dingle temperatures are determined from the field dependence of the dHvA amplitudes. According to Eqs. (2) and (3) a plot $\ln[A\sqrt{H}\sinh(bm_c^* T/m_0 H)]$ vs $1/H$ gives a straight line with slope $-bm_c^* X^*/m_0$. The cyclotron masses used in the analysis are taken from Ref. 20. In the following the influence of electron-phonon interaction on the dHvA amplitudes will be discussed. The electron-phonon interaction changes the dispersion relation $E(\vec{k})$ of the conduction electrons in the vicinity of the Fermi level E_F in the following way[7]:

$$E^*(\vec{k}) - E_F = [E(\vec{k}) - E_F]/[1 + \lambda(\vec{k})] . \tag{5}$$

$\lambda(\vec{k})$ is the electron-phonon enhancement factor which is $\vec{k}$ dependent. The consequences of this change in the dispersion relation on the dHvA effect is shown in Fig. 1. Without electron-phonon interaction neighboring Landau levels are separated by $\hbar\omega_c$ where $\omega_c = eH/m_c c$ is the cyclotron frequency. The levels have a Lorentzian broadening of width $2\pi k_B X$. They are split by the spin into two levels which are separated by $g_c \mu_B H$. As illustrated in Fig. 1, the level separation, the level broadening, and the level splitting are reduced by electron-phonon interaction by a factor $1/(1+\langle\lambda\rangle)$. [$\langle\lambda\rangle$ is the orbital average of $\lambda(\vec{k})$ around the extremal cross section.] Since the temperature damping factor depends on the ratio of the thermal smearing of the Fermi surface $k_B T$ and the separation of neighboring Landau cylinders $\hbar\omega_c/(1+\langle\lambda\rangle)$, it is the enhanced mass $m_c^* = m_c(1+\langle\lambda\rangle)$ that enters this factor. Not so for the Dingle damping factor which depends on the ratio of the level broadening to the level separation. Since both these quantities are diminished by $1+\langle\lambda\rangle$, this factor depends on $m_c^* X^* = m_c X$, which is independent of the electron-phonon interaction. For the same reason the spin splitting factor is independent of $1+\langle\lambda\rangle$.

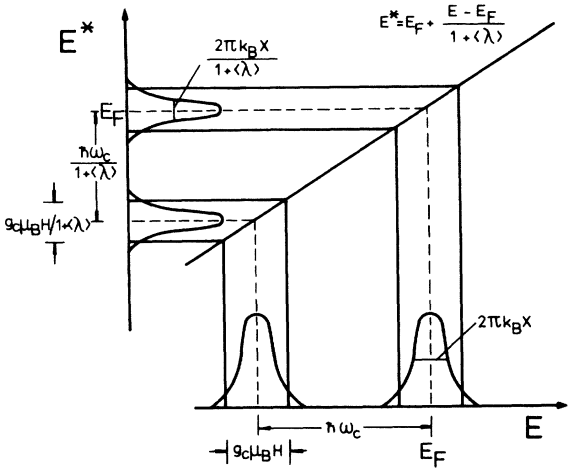

FIG. 1. Plot of E^* vs E in the vicinity of the Fermi level showing the reduction of the Landau-level separation $\hbar\omega_c$, broadening $2\pi k_B X$, and splitting $g_c\mu_B H$ by the factor $(1+\langle\lambda\rangle)^{-1}$ due to electron-phonon interaction. For simplicity the Landau-level broadening is shown only for the not splitted level.

III. EXPERIMENT

A. dHvA apparatus

The dHvA measurements were made in a NbTi superconducting solenoid with a maximum field of 75 kG, using a sample holder which allowed rotation of the sample through 360° about an axis perpendicular to the field. In addition, the sample holder could be tipped through an angle of ±5° about an axis perpendicular to the field and the rotation axis, allowing orientation of the sample in the field to any orientation with an accuracy of a few minutes of arc. The inhomogeneity of the magnetic field was measured with an NMR probe[8] and found to be 5 ppm over the sample volume. Therefore phase smearing due to field inhomogeneity was not a problem. The field modulation method[9] was used with a modulation frequency of 30 Hz to minimize the effect of finite skin depth. Precautions were taken to avoid effects of magnetic interaction and presence of higher harmonic dHvA components.

B. Samples

The samples used in the experiment were cylindrical copper single crystals 1 mm in diam and 5 mm long with the axis of the cylinder in the [110] crystallographic direction. The samples were grown directly as cylinders 1 mm in diam by the Czochralski technique and cut to length by an electrolytic layer saw.[10]

This procedure resulted in samples with an exceptionally low dislocation density of $\simeq 10^3$ cm^{-2} (as shown from counting of etch pits), and corresponding small mosaic spread (<20 arc sec as determined from the width of the Bragg peak using a γ diffractometer with the 412 keV gold line.[11]

TABLE I. Dingle temperature values.

Orbit	X^* (K)
$B\langle 111\rangle$	0.04 ± 0.01
BTP	0.04 ± 0.01
$N\langle 111\rangle$	0.02 ± 0.01
$D\langle 110\rangle$	0.05 ± 0.02
$B51.74$	0.05 ± 0.01
$B65$	0.06 ± 0.01

One of the best tests for the quality of the crystals is the dHvA effect itself. The Dingle temperatures for orbits for which $\partial F/\partial\theta \neq 0$ are very sensitive to small mosaic spreads.[2] Measurements of the Dingle temperatures in the pure samples gave the values which are given in Table I. BTP refers to the belly turning point. B 51.74 and B 65 are "tipped" belly orbits for which $\partial F/\partial\theta \neq 0$ with the field at 51.74° and 65° from the [100] direction, respectively. The low values for the Dingle temperatures of these tipped orbits imply a mosaic spread smaller than 5 arcsec. The residual resistivity of the samples was 0.6 nΩ cm. The samples were loaded with hydrogen by heating in a hydrogen atmosphere at temperatures between 600°C and 730°C and pressures of 4 to 45 atm, and then rapidly quenching to -155 ± 5 °C in an isopentane quench bath.

Because hydrogen dissolves endothermically in copper and is very mobile even at fairly low temperatures, a supersaturated solution tends to precipitate if the hydrogen is mobile. We have investigated the metallurgical behavior of hydrogen in copper[12] by measuring the isochronal and isothermal annealing of the residual resistivity due to the quenched-in hydrogen, together with microscopy studies. This investigation showed that homogeneous solutions of hydrogen in copper can be achieved by rapid quenching to a low temperature where the hydrogen is practically immobile (−150 °C). If, however, the samples are then warmed up, the hydrogen precipitates into bubbles around room temperature. For this reason the dHvA samples were kept below −150 °C after loading with hydrogen until the experiment was completed. In a preliminary report[13] on dHvA measurements of *Cu*H these difficulties were not fully appreciated and the results were probably affected by hydrogen precipitation. The measurements reported in this paper were made on homogeneously loaded samples.

Loading temperatures well below the melting point were used in order to minimize the concentration of vacancies quenched-in with the hydrogen.[14] Since the equilibrium hydrogen concentration c_H is proportional to the square root of the loading pressure, the required hydrogen concentrations could be obtained by loading at higher pressures. In this way the vacancy concentration was kept below about 1% of the hydrogen concentration so that the effect of vacancies could be neglected. The hydrogen concentration in the dHvA samples was determined by measuring the residual resistivity of the samples after the dHvA measurements were completed using the value $\rho_H = 1.50 \pm 0.05$ μΩ cm/at.% for the resistivity of hydrogen in copper. This value was determined by measuring the residual resistivity in single crystalline copper samples loaded with hydrogen in the way described above. The hydrogen content of the samples was then determined directly by outgasing the samples in an evacuated chamber and measuring the pressure rise.[15] The results of the resistivity measurements are shown in Fig. 2. The hydrogen concentration of the dHvA samples was also measured by the heat extraction method but because of their small size this value was less accurate than the value obtained from the resistivity measurement. The value 1.50 μΩ cm/at.% for the resistivity of hydrogen in copper was determined in larger samples (0.25 g) for which the heat extraction results were considerably more accurate because of the greater amount of hydrogen.

C. Dingle temperatures for *Cu*H

Dingle temperatures were measured in 11 samples with hydrogen concentrations ranging from 0 to 140 at. ppm for 11 cyclotron orbits in each sample. Figure 3 shows the data for three typical orbits, the $B\langle 100\rangle$, the $B\langle 111\rangle$, and the $N\langle 111\rangle$. The Dingle temperatures for unit concen-

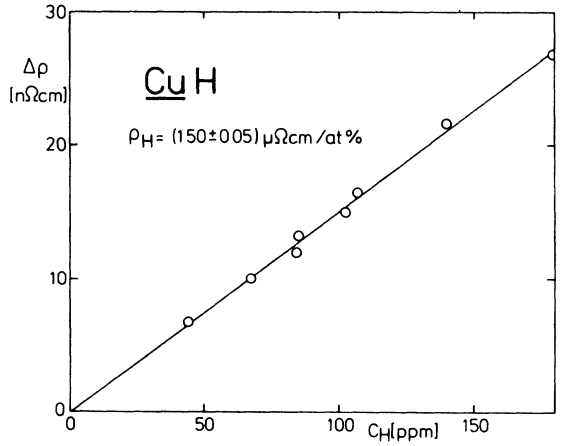

FIG. 2. Residual resistivity of H in Cu. 1 at.% of hydrogen produces a resistivity of (1.50 ± 0.05) μΩ cm at 4.2 K in copper.

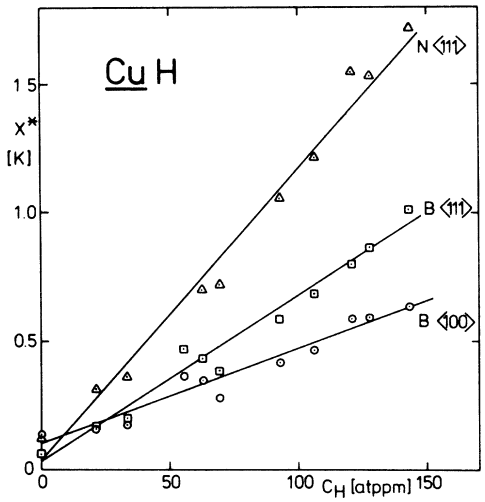

FIG. 3. Dingle temperatures X^* (renormalized by electron-phonon interaction) for three symmetry orbits (neck ⟨111⟩, belly ⟨100⟩, and belly ⟨111⟩) vs hydrogen concentration c_H in Cu. Intercept at $c_H=0$ is due to dislocations produced by the loading of the samples with hydrogen.

tration (1 at.%) were then determined from a least-squares fit to the measured Dingle temperatures versus the hydrogen concentration. It was found that the quenching creates dislocations in the samples. This is clearly shown in Fig. 3 from the data points at zero hydrogen concentration. This sample was quenched under similar conditions as the other samples but replacing the hydrogen by helium gas which is insoluble in copper. The dislocations cause electron scattering which adds to the scattering from the hydrogen. This firstly, gives rise to an intercept on the ordinate of the plots X^* vs c_H (Fig. 3) and secondly causes a scatter of the data. Both effects can only be estimated quantitatively when measurements are made at several different concentrations. For this reason we have analyzed 11 samples with different concentrations of hydrogen. The least-squares fits to the data gave a background scattering of about 0.1 K and rms error for the slope of 5 to 10%.

In Table II the Dingle temperatures per at.% hydrogen are listed for the 11 orbits measured. These Dingle temperatures are renormalized by electron-phonon interaction because the data were deduced from the product $m_c X = m_c^* X^*$ using measured (renormalized) masses m_c^*. Figure 4 shows the paths of the measured orbits folded into the basic $\frac{1}{48}$ zone of the Fermi surface in stereographic projection. The figure shows that the Fermi surface is well covered by these 11 orbits.

IV. DISCUSSION

A. Scattering anisotropy

The large Dingle temperatures for the neck orbits and the much smaller Dingle temperatures for the belly orbits show that the scattering rate is much larger for electrons in states near the neck than for the belly regions of the Fermi surface. This is also seen in the systematic increase in the Dingle temperatures for the belly orbits as the angle between the field and the [100] crystallographic direction is increased, that is, as the orbit comes nearer to the neck (see Fig. 4). The Dingle temperatures for the hole orbits (dogsbones and rosette) fall between the values for the neck and bellies. This is to be expected since these orbits cover both neck and belly regions of the Fermi surface.

In addition, the overall scattering is strong compared to substitutional impurities such as *Cu*Ni or *Au*Zn for which the Dingle temperatures are of the order of 20 to 40 K/at.%,[1,2] or for vacancies in Au (35 to 40 K/at.%).[5]

From the measured Dingle temperatures the local scattering rates can be determined locally over

TABLE II. Measured Dingle temperatures per at.% hydrogen for 11 cyclotron orbits in *Cu*H. *B*, *N*, *D*, and *R* stand for belly, neck, dogsbone, and four-cornered rosette. Numbers in brackets behind the orbit symbol denote the crystallographic directions for the high symmetry orbits. Numbers without brackets give the angle between the field direction and the [001] direction in the plane {110}. BTP refers to the turning point belly 16.2° from [001] in {110}. Errors quoted for X^* are the rms errors of the slope of X^* vs c_H. Systematic errors in the amplitude measurements due to higher dHvA harmonics, magnetic interaction, and skin effect could be kept negligibly small. Cyclotron masses m_c^* quoted in the table are taken from Ref. 20. Both X^* and m_c^* are renormalized by electron-phonon interaction. Fitted Dingle temperatures from the three coefficient fit agree within the experimental errors with the measured values.

		X^* (K/at.%)	
	m_c^*/m_0	Experiment	T_{lmn}
$B\langle 100\rangle$	1.343	37.9 ± 3.0	40.3
B 9	1.320	45.6 ± 3.3	42.9
BTP	1.310	48.4 ± 3.3	48.5
$B\langle 111\rangle$	1.378	65.0 ± 3.7	66.2
B 65	1.431	65.7 ± 8.6	69.4
$N\langle 111\rangle$	0.444	112.6 ± 5.5	112.8
N 65	0.478	102 ± 10	111.9
N 75	0.648	110 ± 13	107.7
$R\langle 100\rangle$	1.307	89.8 ± 8.4	81.7
D 85	1.288	71 ± 13	70.4
$D\langle 110\rangle$	1.260	77.3 ± 6.7	70.0

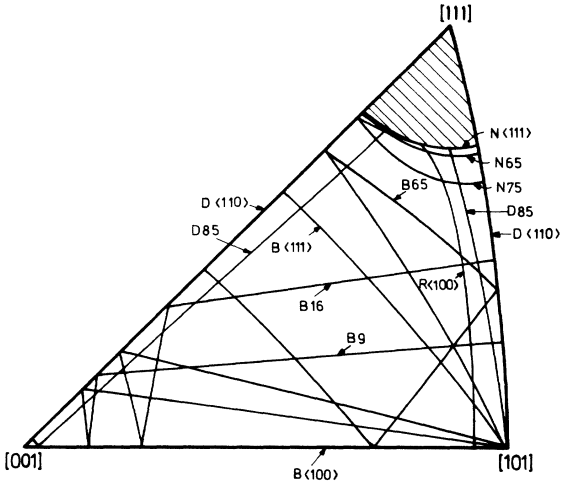

FIG. 4. Trajectories over the Fermi surface of the 11 orbits measured, shown as stereographic projections of the $\frac{1}{48}$ unit of the Fermi surface. Notation of the orbits is as in Table II.

the Fermi surface. The orbital average of the local scattering rates (and hence the Dingle temperature) can be expressed as an integral of the local scattering rates around an orbit weighted by the time spent at each point on the orbit[2]

$$\left\langle \frac{1}{\tau^*} \right\rangle = \oint \frac{1}{\tau^*(\vec{k}) v_\perp^*} d\vec{k} \Big/ \oint \frac{1}{v_\perp^*} d\vec{k} , \qquad (6)$$

where $v_\perp^*$ is the component of the Fermi velocity perpendicular to the field direction.

As a representation for $1/\tau^*(\vec{k})$ we have used the symmetrized Fourier series described by Lowndes *et al.*[2]:

$$\frac{1}{\tau^*(\vec{k})} = \sum_{l,m,n} T_{lmn} \cos\left(\frac{lak_x}{2}\right) \times \cos\left(\frac{mak_y}{2}\right) \cos\left(\frac{nak_z}{2}\right) , \qquad (7)$$

with $l+m+n$ even, a is the lattice parameter, and T_{lmn} are the coefficients to be determined. The summation includes permutations of x, y, and z.

Using Eq. (6) and the representation [Eq. (7)] for the local scattering rate, the coefficients T_{lmn} were fitted to the measured Dingle temperatures for *Cu*H using various numbers of terms in the Fourier series. It was found that for an adequate fit at least three coefficients were required but that using more than three coefficients did not significantly improve the fit. Further, as the number of coefficients increases, the standard error in the local scattering rates increases because of increasing correlation between the Fourier terms, so that a three coefficient fit is in fact the most significant fit. In the present analysis we have used the Cu5 representation of Halse[16] for the Cu Fermi surface and a five coefficient Fourier representation for the Fermi velocities obtained from our recent cyclotron mass measurements which will be reported in a subsequent publication.[20]

The coefficients to Eq. (7) for the local scattering rates are given in Table III. The fitted Dingle temperatures given in Table II agree within the experimental error with the measured values. Contour plots of the local scattering rates and the corresponding standard error from this fit are shown in Fig. 5 over the basic $\frac{1}{48}$ zone of the Fermi surface. This picture quantitatively shows what could be seen qualitatively directly from the Dingle temperatures: the scattering is strongest at the neck and decreases away from the neck to lower values in the belly regions.

B. Phase-shift analysis of electron scattering from H in Cu

The origin of the scattering anisotropy can be seen more quantitatively from a phase-shift analysis based on a Korringa–Kohn–Rostoker band-structure model recently developed by Holzwarth, Lee, and Coleridge[17–19] for dilute noble-metal alloys. In this theory the waves scattered by the defect are not plane waves but the Bloch waves appropriate to the host lattice in which the defect is imbedded. The model uses the muffin-tin approximation both for the host lattice and for the defect. The essential new aspect introduced by the crystal is that in addition to the phase shift $\Delta\eta_l$ between the incident and scattered wave caused by the defect, the incident wave already includes a phase shift θ_L caused by backscattering of the scattered wave from the surrounding lattice. The scattering is therefore parametrized by the total phase shift caused by the defect. The total phase shift $\phi_L = \Delta\eta_l + \theta_L$ is called the Friedel phase shift. In the case of hydrogen in Cu, which presumably occupies octahedral interstitial lattice sites, $\Delta\eta_l$ is just the phase shift η_l^i due to the hydrogen scattering potential. Since the backscattered wave has the point symmetry of the defect site, the different phase shifts are labeled by $L = l$, Γ, where l is the angular momentum and Γ are the representations of the

TABLE III. Scattering rate coefficients T_{lmn} [in units of 10^{13} sec^{-1} (at.%)$^{-1}$] from a three-term symmetrized Fourier series [Eq. (7)].

	T_{lmn} (10^{13} sec^{-1} at.%$^{-1}$)
000	−2.004
110	−19.041
200	−3.601

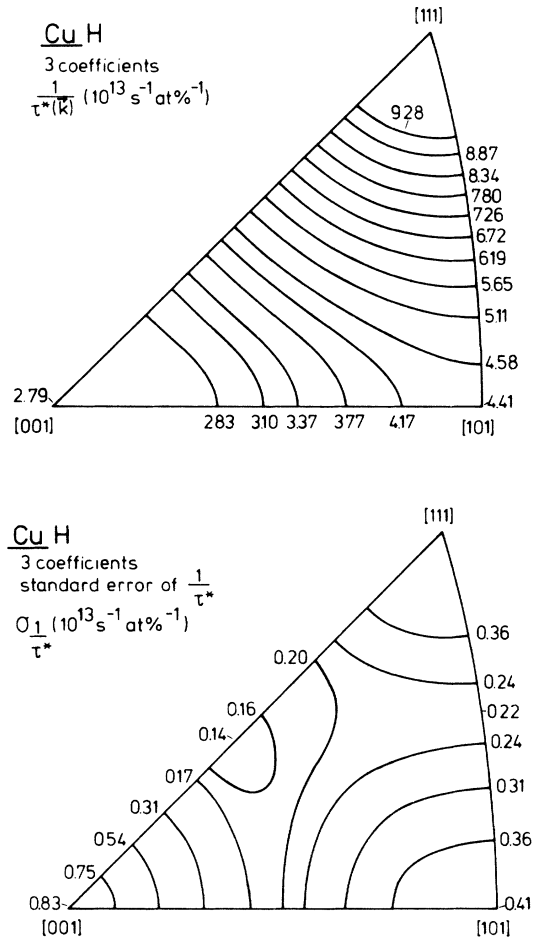

FIG. 5. Local values of the scattering rates $1/\tau^*(\vec{k})$ for *Cu*H in the basic unit of the Fermi surface using a three coefficients symmetrized Fourier series to fit the experimental data of Table II. σ_{1/τ^*} is the standard error of the local scattering rates. Scattering is strongest at the neck, decreasing monotonically towards the belly point [001].

point group belonging to the different l. The ϕ_L have to fulfill the Friedel sum rule which reads

$$\sum_L 2g_L \frac{\phi_L}{\pi} = \Delta Z \,, \tag{8}$$

where g_L is the degeneracy of the representation, l, Γ and ΔZ is the effective charge to be screened by the electrons. The Dingle temperatures can be expressed in a nonrelativistic treatment in terms of the Friedel phase shifts as[18]

$$\frac{X^* m_c^*}{m_0} = c_H \left(\frac{a_0}{a}\right)^2 \frac{\epsilon_0}{k_B} \sum_L \frac{W_L}{\mathrm{Im}\chi_L} \sin^2\phi_L \,, \tag{9}$$

with $\epsilon_0 = 1$ Ry, k_B is Boltzmann's constant, a is the lattice parameter, and a_0 is the Bohr radius. The Dingle temperatures are decomposed in lattice harmonics contributions L. Terms with $l > 2$ are neglected. The parameters W_L are orbital averages of the $\vec{k}$-dependent part of the T matrix belonging to different L. They depend only on host lattice properties and have been calculated for a certain number of orbits for substitutional and octahedral interstitial defects in the noble metals.[18,19] The information on the defect is contained in the factors $\sin^2\phi_L$. The Brillouin-zone integrals χ_L describe how a scattered wave diverging from the defect contributes to the amplitude at the defect site due to backscattering from all the host sites. The χ_L depend on the host lattice and on the position of the defect in the lattice but not on the scattering strength of the defect. They have also been calculated for substitutional and octahedral interstitial defect sites in the noble metals.[18,19] The scattering strength of the defect enters into the Friedel phase shifts ϕ_L. For an octahedral interstitial defect like H in Cu it is

$$\tan\phi_L = \mathrm{Im}\chi_L / (\cot\eta_l^i - \mathrm{Re}\chi_L) \,. \tag{10}$$

Hence the representation [Eq. (9)] of the Dingle temperatures can be looked at in the following way. The anisotropy of the scattering of the different lattice harmonics waves L depends only on the host lattice and on the position of the defect. The weight by which the anisotropies of the different contributions L superpose to form the resultant anisotropy (as measured in the Dingle temperatures) is given by host properties, by the position of the defect, *and* by the scattering strength of the defect. With this interpretation in mind and the values of the parameters W_L from Ref. 18 it can be seen immediately that a defect well localized at an octahedral interstitial site in Cu (i.e., defect with $\eta_0^i \neq 0$ but $\eta_1^i = \eta_2^i = \cdots = 0$) produces the highest Dingle temperatures for the $N\langle 111\rangle$ and the smallest for the $B\langle 100\rangle$. This is just what has been observed in our experiment. We therefore expect strong s scattering of the electrons from hydrogen in Cu. The phase shifts were fitted to the measured Dingle temperatures using Eq. (9). Since the orbital coefficients W_L have only been calculated for the six orbits with $\partial F/\partial\theta = 0$, only these orbits were used in the fit. Table IV gives the phase shifts and the fitted values of the Dingle temperatures. The fitted values agree quite well with the experimental data although the fit is not as good as the Fourier fit (Table III). Since the ϕ_L enter the fit quadratically, their sign cannot be determined from the Dingle temperatures alone. The possible combinations of the ϕ_L give Friedel sums [Eq. (8)] of $\pm(0.88 \pm 0.06)$ and $\pm(0.42 \pm 0.09)$.

The effective charge ΔZ to be screened by the conduction electrons is

TABLE IV. Phase-shift analysis of the data given in Table I. Friedel phase shifts ϕ_L and the impurity phase shifts η_l^i are largest for the wave $L=0, \Gamma 1$. This reflects the short range of the hydrogen scattering potential located at an octahedral interstitial site. In the fit only the orbits with $\partial F/\partial\theta = 0$ were utilized.

	ϕ_L	η_l^i	θ_L
$s\Gamma_1$	1.032 ±0.035	1.641	−0.609
$p\Gamma_{15}$	0.115 ±0.037	0.152	−0.037
$d\Gamma_{12}$	0	0	0
$d\Gamma_{25}$	0	0	0

X^* (K/at.%)	Experiment	Fit
$B\langle 100\rangle$	37.9 ± 3.0	40.3
BTP	48.4 ± 3.3	48.4
$B\langle 111\rangle$	65.0 ± 3.7	61.2
$D\langle 110\rangle$	77.3 ± 6.7	68.7
$R\langle 100\rangle$	89.8 ± 8.4	78.5
$N\langle 111\rangle$	112.6 ± 5.5	120.7

$$\Delta Z = 1 - (\Delta V/V)_{\text{loc}} \,. \tag{11}$$

The correction term $(\Delta V/V)_{\text{loc}}$ takes into account the influence of the local relaxation of the lattice around the proton on the screening charge. In a first approximation it is[21]

$$\left(\frac{\Delta V}{V}\right)_{\text{loc}} = \frac{1}{3}\,\frac{1+\nu}{1-\nu}\,3\,\frac{\Delta a}{a} \,, \tag{12}$$

with the Poisson number $\nu = 0.32$ for Cu.[30] The lattice parameter change $\Delta a/a$ has not been measured in the system *Cu*H. To get the right order of magnitude the value for PdH can be taken. $\Delta a/a$ was found for this system to be $+5.7\times10^{-4}$ at.%.[22] This gives $(\Delta V/V)_{\text{loc}} = 0.11$ and $\Delta Z = 0.89$. The Friedel sum of +0.88 agrees very well with ΔZ. We conclude that the correct combination of signs of the phase shifts is the one given in Table IV. Once the ϕ_L are known, the phase shifts η_l^i of the hydrogen potential and the backscattering phase shift θ_L can be calculated according to Eq. (10) and to the relation

$$\phi_L = \eta_l^i + \theta_L \,. \tag{13}$$

The values for η_l^i and θ_L deduced from the fitted values ϕ_L are given in Table IV. The table shows that the s phase shift is the dominant one, that the p phase shift is an order of magnitude smaller and that the d phase shift is negligible. This means that the scattering potential of the dissolved hydrogen in Cu is short ranged compared to the de Broglie wavelength of the conduction electrons at the Fermi level.

The following conclusions can be made from the analysis given here. The phase-shift analysis by Coleridge, Holzwarth, and Lee explains in an elegant way the origin of the observed anisotropy of the scattering rates. It is the short range of the hydrogen potential and its location at the octahedral interstitial site in Cu which is responsible for the strong neck scattering and the weaker $B\langle 100\rangle$ scattering. Although the s-phase shift η_0^i is the dominant one, it is necessary to include a small p-phase shift η_1^i to obtain quantitative agreement between theory and experiment.

A second point should be emphasized. It is a well-established fact that the hydrogen in Cu occupies interstitial lattice sites.[12] But up to now it has not yet been shown experimentally if the hydrogen occupies octahedral interstices as it was assumed in this analysis. In principle tetrahedral interstices [at $(\frac{1}{4}a, \frac{1}{4}a, \frac{1}{4}a)$] could be occupied as well. We believe that the observed scattering anisotropy is not consistent with the occupation of tetrahedral sites. In fact, it can be seen from band-structure calculations[27] that states $\vec{k}$ which contribute to the $B\langle 100\rangle$ orbit have s character about the tetrahedral interstices of similar magnitude to those from the neck. Hence the Dingle temperatures for the $B\langle 100\rangle$ and the $N\langle 111\rangle$ orbits should be similar in magnitude in contrast to the experimental result. Therefore the observed anisotropy can be considered as a strong indication that the hydrogen indeed occupies octahedral interstices in Cu as assumed throughout this paper. To make this structure analysis more quantitative it would be necessary to calculate the host orbital parameters W_L and the Brillouin-zone integrals χ_L for tetrahedral interstitials in Cu.

C. Calculation of local scattering rates for *Cu*H by the average-t-matrix approximation

Local scattering rates and Dingle temperatures have recently been calculated for hydrogen in Cu by Huisman and Weiss.[23] Their calculation was based on an average-t-matrix approximation (ATA) for nondilute alloys used by Bansil *et al.*[24] to calculate the complex energy bands in α-brass. For Cu these authors have chosen a renormalized atom potential[25] confined to touching muffin-tin spheres. The potential for the occupied octahedral interstitial sites was[26]

$$V(r) = e/r - V_0, \quad r \le r_{\text{H}} = 0.9971\, a_0 \,. \tag{14}$$

$V_0 = -0.829$ Ry is the average of the Cu potential in the volume outside the Cu muffin-tin spheres (with the zero of potential taken at infinity). The phase shifts were calculated at $E_F = 0.685$ Ry which is their assumed values of the Fermi energy for pure

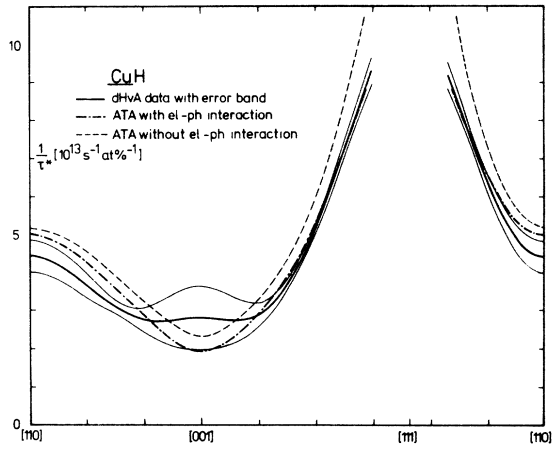

FIG. 6. Local values of the scattering rates for *Cu*H calculated by ATA [Huisman and Weiss (Ref. 23)] without and with electron-phonon interaction. Local values $1+\lambda(\vec{k})$ were taken from Ref. 20. Accuracy of the calculated data is $\pm 0.4\times 10^{13}$ sec^{-1} (at.%)$^{-1}$. Excellent agreement is found between the theoretical data and the experimental data given by Eq. (7) and the coefficients of Table III.

Cu relative to V_0. The values obtained were[28]

$$\eta_0^i = 1.353, \quad \eta_1^i = 0.025, \quad \eta_2^i = 0. \tag{15}$$

It should be noted that these phase shifts are significantly smaller than the values obtained from our Dingle temperatures (Table IV). Values for the scattering rates calculated in this model for *Cu*H are shown in Fig. 6. These results do not include electron-phonon interaction and are therefore not immediately comparable with the dHvA results. We have therefore divided the results of Huisman and Weiss by the factor $[1+\lambda(\vec{k})]$ as deduced from our cyclotron mass measurements.[20] The renormalized scattering rates from the ATA calculation are shown in Fig. 6 together with our measured data. The anisotropy of the calculated scattering rates is in excellent agreement with the experiment. This is a consequence of the choice of the potential [Eq. (14)] which is short ranged, because it is confined to a small muffin-tin sphere and which consequently produces mainly s-phase shifts. It is noteworthy that in addition to the correct scattering anisotropy, the ATA calculation also gives absolute values which agree very well with the experimental data within the error limits. However, if the hydrogen phase shifts η_l^i by Huisman and Weiss [Eq. (15)] are used to calculate Dingle temperatures with the phase shift formalism by Holzwarth and Lee [Eq. (9)],

TABLE V. Dingle temperatures X^* (including electron-phonon interaction) for *Cu*H calculated by ATA and by phase-shift analysis with the same set of hydrogen phase shifts η_l^i ($\eta_0^i = 1.353$, $\eta_1^i = 0.025$, $\eta_2^i = 0$).[28]

X^* (K/at.%)	Experiment	ATA	Phase-shift analysis
$B\langle 100\rangle$	37.9 ± 3.0	41	24.6
$D\langle 110\rangle$	77.3 ± 6.7	74	45.1
$N\langle 111\rangle$	112.6 ± 5.5	114	82.6

then it turns out that the data are too small by a factor of about 1.5 compared to the experimental results (Table V). So there is a discrepancy between the two descriptions of the scattering which may be due to the following reasons. The first is the different choice of band-structure parameters for Cu (Fermi energy and muffin-tin zero) used in the phase-shift analysis and in the ATA calculation. This could be checked by repeating the ATA calculation using the same band-structure parameters for Cu as used by Holzwarth and Lee. It should be noted that the parameter set used by Holzwarth and Lee fits the known Fermi-surface geometry much better than the set used by Huisman and Weiss. The discrepancy could also be due to the way in which backscattering is included in the two models. Since the phase shift θ_L introduced by backscattering is large ($\theta_0 = -35°$, Table IV), this is an important effect. In the phase-shift analysis the backscattering is treated correctly (as long as lattice distortion around the defect can be neglected). It is not clear how far this is true as well for the ATA. This point has been somewhat controversial in previous publications.[29] The proposed ATA calculation with the band-structure parameters used by Holzwarth *et al.* may help to elucidate this problem.

ACKNOWLEDGMENTS

We are grateful to Dr. N. A. W. Holzwarth and Dr. R. O. Jones, to Professor H. Ehrenreich and to Dr. C. D. Gelatt and Dr. L. Huisman for helpful discussions and for making their results available to us prior to publication. We are greatly indebted to Dr. W. Uelhoff, Mr. M. Abdel-Fattah, and G. Hanke for supplying us the single crystals used in this analysis and to Mr. H. J. Fenzl for checking the crystal quality with his γ-diffractometer. Finally we would like to express our special gratitude to Professor W. Schilling for his continuous support of our dHvA work.

*Present address: Div. 5111, Sandia Laboratories, Albuquerque, N. M. 87115.
[1]M. Springford, Adv. Phys. 20, 493 (1971).
[2]D. L. Lowndes, K. M. Miller, R. G. Poulsen, and M. Springford, Proc. R. Soc. A 331, 497 (1973).
[3]H. R. Brown and A. Myers, J. Phys. F 2, 683 (1972).
[4]R. G. Poulsen, D. L. Randles, and M. Springford, J. Phys. F 4, 981 (1974).
[5]B. Lengeler, W. Uelhoff, Phys. Lett. A 53, 139 (1975); and unpublished.
[6]A. V. Gold, in *Solid State Physics*, edited by J. F. Cochran and R. R. Hearing (Gordon and Breach, New York, 1968), Vol. 1.
[7]J. W. Wilkins, *Observable Many-body Effects in Metals*, NORDITA, 1968 (unpublished).
[8]W. R. Wampler, S. Matula, B. Lengeler, and G. Durcansky, Rev. Sci. Instrum. 46, 581 (1975).
[9]D. Shoenberg and P. J. Stiles, Proc. R. Soc. A 281, 62 (1964).
[10]M. Abdel-Fattah, V. Sorajić, and W. Uelhoff, Jülich Report JÜL-944-FF (1973) (unpublished).
[11]H.-J. Fenzl (private communication).
[12]W. R. Wampler, T. Schober, and B. Lengeler, Philos. Mag. 34, 129 (1976).
[13]B. Lengeler and W. R. Wampler, in *Low Temperature Physics LT13*, edited by K. D. Timmerhaus, W. J. O'Sullivan, E. F. Hammel (Plenum, New York, 1974), Vol. 4, p. 173.
[14]R. R. Bourassa and B. Lengeler, J. Phys. F 6, 1405 (1976).
[15]B. Lengeler, K.-H. Klatt, and W. R. Wampler, Technical information of the KFA Jülich, Report No. 8 (1976) (unpublished).
[16]M. R. Halse, Philos. Trans. Roy. Soc. Lond. A 265, 507 (1969).
[17]P. T. Coleridge, N. A. W. Holzwarth, and M. J. G. Lee, Phys. Rev. B 10, 1213 (1974).
[18]N. A. W. Holzwarth and M. J. G. Lee, Phys. Kondens. Mat. 19, 161 (1975).
[19]M. J. G. Lee, N. A. W. Holzwarth, and P. T. Coleridge, Phys. Rev. B 13, 3249 (1976).
[20]B. Lengeler, W. R. Wampler, R. R. Bourassa, K. Mika, K. Wingerath, and W. Uelhoff (unpublished).
[21]F. J. Blatt, Phys. Rev. 108, 285 (1957).
[22]E. Wicke and G. H. Nernst, Z. Elektrochem. 68, 224 (1964).
[23]L. Huisman and J. A. Weiss, Solid State Commun. 16, 983 (1975).
[24]A. Bansil, H. Ehrenreich, L. Schwartz, and R. E. Watson, Phys. Rev. B 9, 445 (1974).
[25]L. Hodges, R. E. Watson, and H. Ehrenreich, Phys. Rev. B 5, 3953 (1972).
[26]H. Ehrenreich, C. D. Gelatt, and L. Huisman (private communication).
[27]B. Segall, Phys. Rev. 125, 109 (1962).
[28]H. Ehrenreich, C. D. Gelatt, and L. Huisman (unpublished).
[29]A. Bansil, L. Schwartz, and H. Ehrenreich, Phys. Kondens. Mat. 19, 391 (1975).
[30]P. H. Dederichs and J. Pollmann, Z. Phys. 255, 315 (1972).